

# Effect of tin on deformation and microstructures of $\alpha$ titanium alloys

YINZE JI<sup>a,\*</sup>, CHAO YIN<sup>b</sup>

<sup>a</sup>*School of Materials, University of Manchester, Great Britain*

<sup>b</sup>*College of Energy and Electrical Engineering, Hohai University, China*

In this work the effect of chemistry on mechanical behaviour of  $\alpha$  titanium alloys was investigated. Optical microscopy, X-ray diffraction and electron backscatter diffraction were used to characterise the microstructure and texture development during quasi-static compression test in rolling direction, normal direction and 45°. The effect of tin concentration on lattice constant and how microstructure and texture change with content of tin was looked into.

(Received December 2, 2013; accepted September 11, 2014)

*Keywords:* Tin, Titanium, mechanical tests, Texture, Lattice constant

## 1. Introduction

Titanium alloys are found massively in earth crust, accounting for about 0.6%. Therefore titanium is considered the fourth most common metallic structural material after aluminium, iron, and magnesium [1].

Properties of titanium alloys depend on composition (i.e. content of alloying elements) and its processing history. What has been widely accepted is that the difference in microstructure and texture are generated by thermal and mechanical treatments [2].

The crystal structure in titanium in low temperature is hexagonal close packed (HCP) and therefore the number of slip systems is limited. Hence, twinning has a great importance in titanium alloys during deformation. Alloying elements are known to greatly affect twin nucleation and growth such as tin [3].

Titanium alloys are strengthened when alloyed with tin, aluminium or zirconium. However the ductility decreases as a result of the solid solution strengthened mechanism [4]. Solid solution strengtheners like tin aluminium and zirconium will cause a lattice distortion, which means an increase of critical resolved shear stress (CRSS) for the different deformation systems, leading to a relative change between the deformation mechanisms. Due to the strengthening effect, tin, aluminium and zirconium are commonly used as alloying compositions in  $\alpha$  titanium alloy [4].

Because of the influence of twinning on the mechanical properties of titanium alloys, it is quite important to understand the elements which will affect twinning and how the properties are evolved from commercially pure titanium to binary Ti-Sn alloys.

## 2. Materials and methods

The materials used are CPTi (commercially pure titanium annealed at 700°C for 5 hours), Ti<sub>2</sub>Sn (titanium alloy with 2.5wt% tin annealed at 860°C for 8 hours) and Ti<sub>8</sub>Sn (titanium alloy with 8.24wt% tin annealed at 860°C for 25 hours). All samples are divided into three categories according to the orientation: rolling direction (RD), 45° and normal direction sample (ND).

A series of compression tests were carried out. The compression samples were made cylinders with an original size of 9±0.1mm in length and 6±0.04mm in diameter. All the samples were compressed to a strain of about 1.7%, 3.7% or 8.7%. Micrographs of all the samples were captured using the same settings to compare the change in microstructures after a certain level of strain including the initial state. Also development of twin area fraction of each alloy under different strains is tracked using the point count technique. Points were put in the pictures and the ones located in the twin (including the twin boundaries) were counted to calculate the twin area fraction. At the same time, lattice constant and textures at different compression stages are obtained and compared to analyse the evolution of microstructure.

## 3. Results

### 3.1 Stress-strain curves

As Fig. 1-3 show, in rolling direction Ti<sub>8</sub>Sn has the highest yield point and the material gets softer with lower tin concentration. Pure titanium shows the lowest work hardening rate while Ti<sub>2</sub>Sn and Ti<sub>8</sub>Sn behave similar and the work hardening rate is higher. Both Ti<sub>2</sub>Sn and Ti<sub>8</sub>Sn

show a much higher yield stress in 45° and they are quite similar but Ti<sub>8</sub>Sn is slightly higher. The work hardening rate of Ti<sub>2</sub>Sn and Ti<sub>8</sub>Sn are similar as they share a similar slope after yield point. Work hardening rate of pure titanium is the lowest. From the ND sample curves, Ti<sub>8</sub>Sn shows the highest yield point, Ti<sub>2</sub>Sn medium and pure titanium the lowest. The work hardening rate increases with tin concentration as the slope after yield point for Ti<sub>8</sub>Sn is the highest and pure titanium is the lowest.

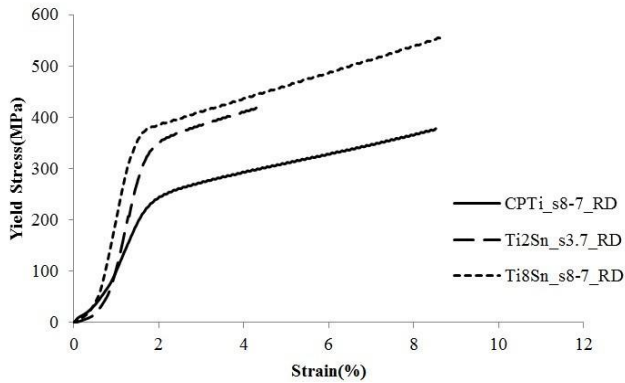


Fig. 1. Stress-strain curves in RD.

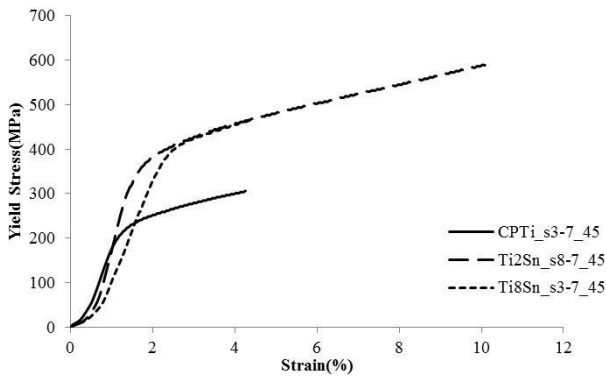


Fig. 2. Stress-strain curves in 45°.

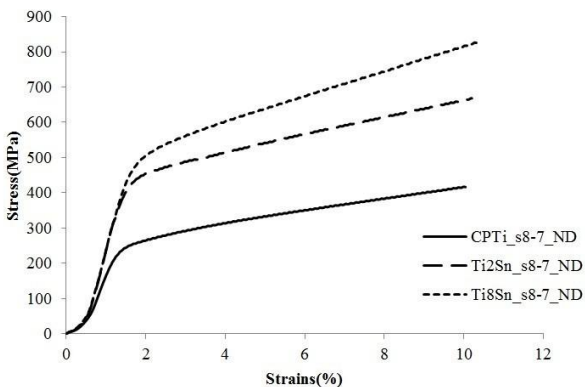


Fig. 3. Stress-strain curves in ND.

From all the stress-strain curves above, the yield point of each sample in different directions can be derived as the

yield point is the stress at 0.2% plastic strain. And the results are shown below in Table 1.

Table 1. Yield points of all the samples (MPa).

	CP titanium	Ti <sub>2</sub> Sn	Ti <sub>8</sub> Sn
ND	243	416	478.5
45°	225	351.5	407
RD	214	331	369.5

For all the samples, yield stress in three different orientations is similar with a maximum deviation of 60MPa. As the three stress-strain curves above show, yield stress and work hardening rate both increase as tin concentration.

### 3.2 Optical microscopy

Microstructures of each alloy before and after compression were investigated and compared. Large amount of twins appeared after compression and the area fraction of twin was calculated roughly and the results are shown in Fig. 4-6.

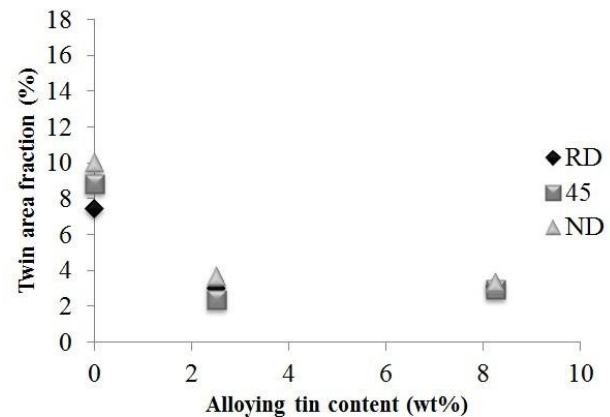


Fig. 4. Twin area fraction after 1.7% strain.

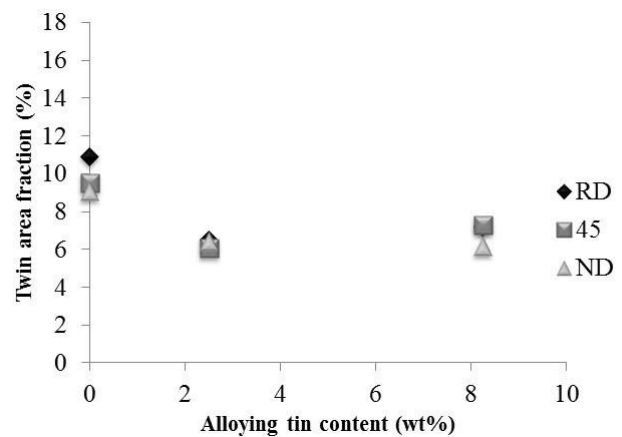


Fig. 5. Twin area fraction after 3.7% strain.

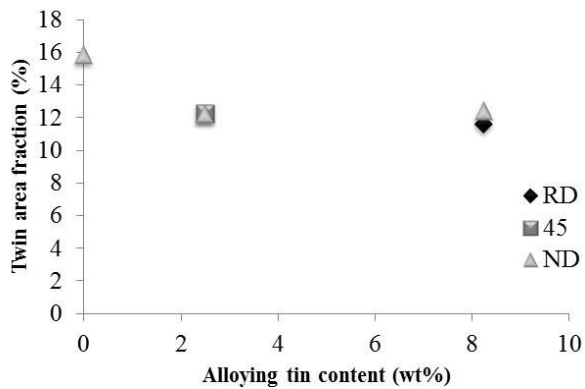


Fig. 6. Twin area fraction after 8.7% strain.

For each material, twin area fraction increases with higher strain. Many twins emerge during deformation.

All these three figures show the same trend of twin

activity at a particular strain level. Twin area fraction decreases at first between pure titanium and Ti<sub>2</sub>Sn and then remains nearly constant after 2.5wt% tin. Orientation effect here is not obvious. For each alloy, twin area fraction doesn't differ much from each other in three directions.

### 3.3 Lattice constant

Lattice constant is a very important value in determining the micro-structure of materials. And lattice constant is related to many basic properties of material like elastic coefficient, thermal expansion and so on [5]. Lattice constant can be measured using techniques like X-ray diffraction or neutron diffraction [6]. In this project, X-ray diffraction of different planes was applied to calculate lattice constant to get reasonable scatters and more convincing results and the peaks are shown in Fig. 7-9.

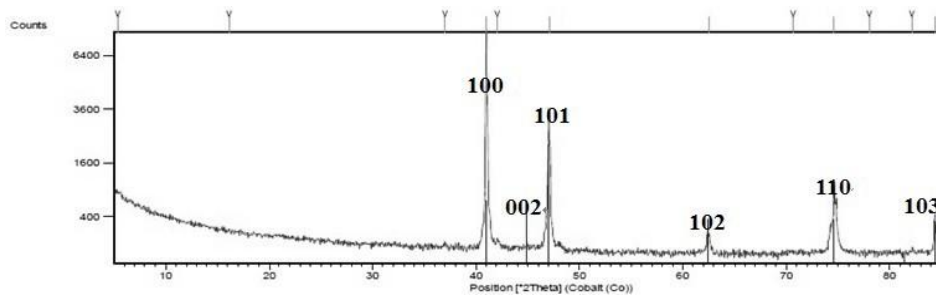


Fig. 7. XRD profile of CPTi in RD.

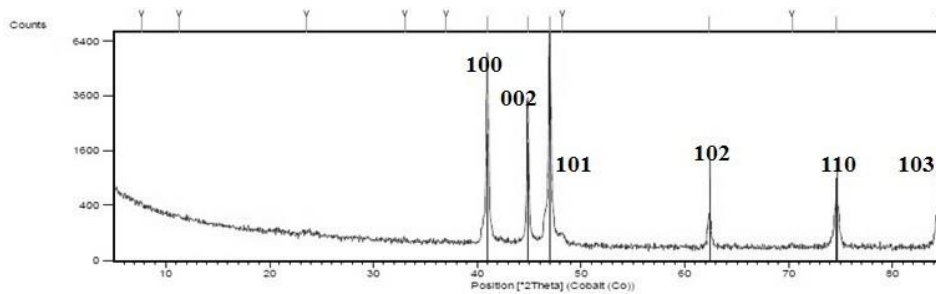


Fig. 8. XRD profile of Ti<sub>2</sub>Sn in RD+ND.

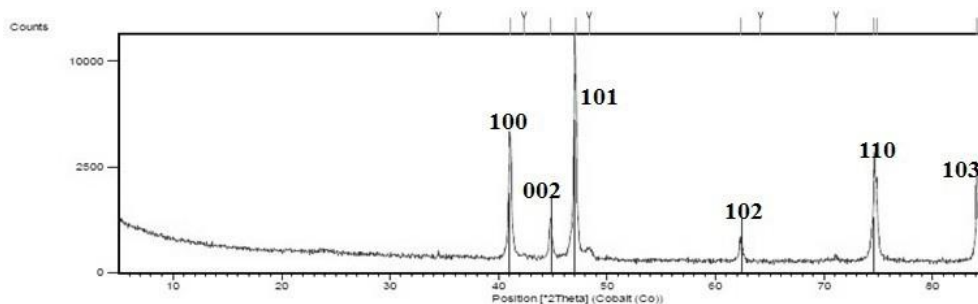


Fig. 9. XRD profile of Ti<sub>8</sub>Sn in RD+ND.

The peaks of all these three alloys stay nearly the same positions. Strong reflection of (0002) planes is observed when sample in normal direction is included. The reason is that in rolling direction sample, c-axis is parallel to the reflecting surface while nearly all basal planes are perpendicular to reflecting surface. This leads to weak intensity of (0002) reflection in sample in rolling direction.

There are tiny peaks at about  $23^\circ$  and  $48.5^\circ$  in each profile. And they're growing more obvious with higher tin concentration. Yet no conclusions about what they are can be drawn. Some more tests are required to figure out.

Both X-ray and neutron diffraction can measure the distance between different planes (d-spacing). Mathematical calculations are required to extract the lattice constant ( $\langle a \rangle$  and  $\langle c \rangle$  for hexagonal close-packed structure). All the formulas used to calculate lattice constant are listed in Table 2.

Table 2. Formulas used to extract lattice constant in titanium alloys.

d-spacing	Formulas
100 planes	$a = \frac{d}{\sqrt{3}} \times 2$
002 planes	$c = d \times 2$
101 planes	$c = \tan\left(\sin^{-1} \frac{2d}{\sqrt{3}a}\right) \times \frac{\sqrt{3}a}{2}$
102 planes	$c = \tan\left(\sin^{-1} \frac{2d}{\sqrt{3}a}\right) \times \sqrt{3}a$
110 planes	$a = d \times 2$
103 planes	$c = \tan\left(\sin^{-1} \frac{2d}{\sqrt{3}a}\right) \times \frac{3\sqrt{3}a}{2}$

The lattice constant of titanium alloys is shown in Fig. 10. In X-ray diffraction, lattice constant  $\langle a \rangle$  stays nearly equal with increasing tin concentration. For lattice constant  $\langle c \rangle$ , the increasing trend slows down after 2.5wt% tin. However, X-ray diffraction shows by trend increasing  $\langle c \rangle$  with increasing tin concentration despite the high scatters.

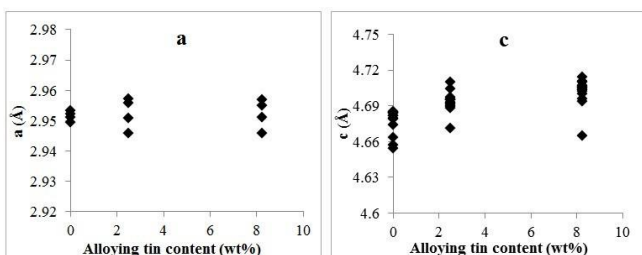


Fig. 10. Lattice constant from XRD.

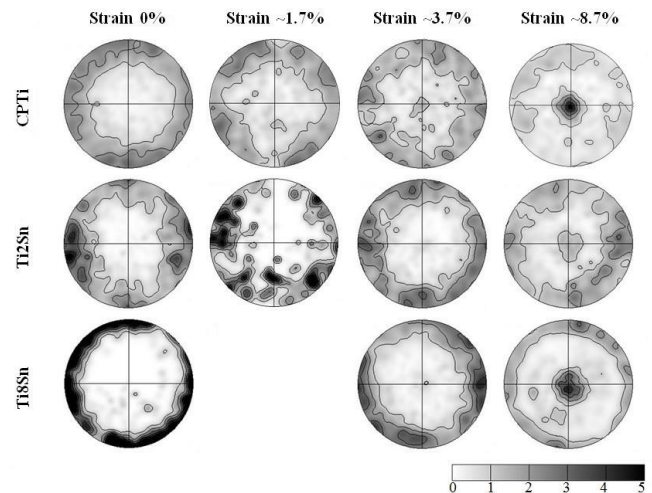
The  $c/a$  ratio is calculated. An increasing trend is observed with higher tin concentration. This is mainly because of the increase of  $\langle c \rangle$  value while  $\langle a \rangle$  value stays nearly constant.

### 3.4. Texture evolution

Texture has been widely used to characterize grain orientation in metal and can be determined by many methods [8]. Here in this project, electron backscattered diffraction was applied.

Texture evolution for CPTi,  $Ti_2Sn$  and  $Ti_8Sn$  in rolling direction at different strain levels is depicted in Table 3 below.

Table 3. 0002 pole figures of different alloys in RD at four strain levels.



Texture evolution trend can be observed. At 0% strain, all three materials have similar texture. As deformation strain level goes higher, black dots emerge at the centre of the pole figures, which indicates that some grains have turned about  $90^\circ$ . This trend is quite similar for all three alloys but the strain required to generate this rotation is not exactly the same. For pure titanium, the central black dots are quite clear when deformation strain reaches 3.7%. However for  $Ti_2Sn$  and  $Ti_8Sn$ , they behave quite similar as there are only little clusters or shaded areas in the centre. As strain keeps increasing, central cluster grows bigger and becomes most obvious at 8.7% strain.

## 4. Discussion

### 4.1. Compression tests

The yield points derived from the mechanical curves are shown in Fig. 11 as function of alloying tin content.

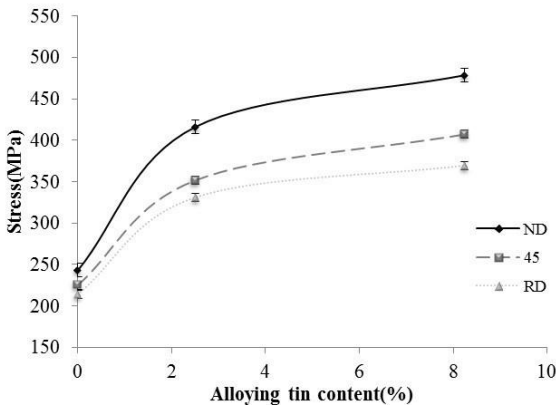


Fig. 11. Yield point of different samples.

An average increase of 139MPa in yield stress is observed between CP titanium and Ti<sub>2</sub>Sn. When the tin content increases from 2.5wt% to 8.24wt%, the yield stress increases by 52MPa in average, which is about one third of the difference between CP titanium and Ti<sub>2</sub>Sn.

For CP titanium, Ti<sub>2</sub>Sn and Ti<sub>8</sub>Sn, the yield stress of 45° samples are always close to the samples in rolling direction.

4.2. Lattice constant

For titanium-tin alloying system, the lattice constant profile is available below in Fig. 3-2-3. Lattice constant of tin comes from [5].

According to Vegard’s law, the lattice constant of titanium-based alloy should increase with the introduction of tin atoms as the dashed lines show in Fig. 12, while the observed behaviour is not increasing remarkably. There is a negative deviation in titanium-rich region.

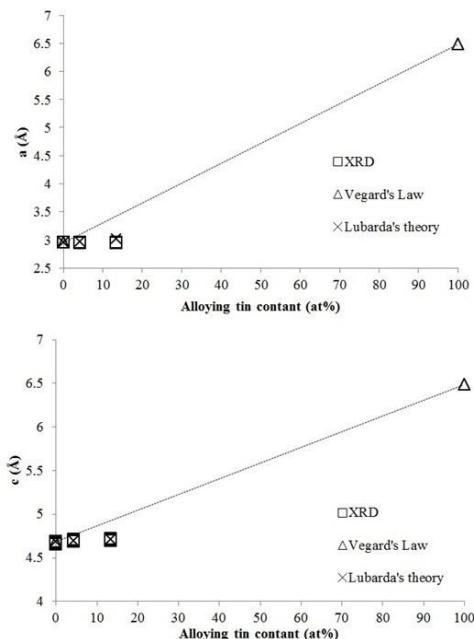


Fig. 12. Approximation of lattice constant.

Lubarda suggests a better fit of lattice constant as Equation 1.

$$a = [a_1^3 + 4\pi R_1^3 x \frac{k_1}{\theta_1} \gamma C]^{\frac{1}{3}} \cdot [\frac{k\theta_1}{k_1\theta}]^{\frac{1}{3}} \quad \text{Equation 1,}$$

In titanium-tin alloying system,  
 $a_1 = 2.9506\text{Å}$ , lattice constant of pure titanium,  
 $R_1 = 1.6153\text{Å}$ , atomic radius of titanium,  
 $x = 4.228\%$  and  $13.390\%$  respectively, atomic percentage of tin in titanium,  
 $k = k_1 = 6$ , atomic number per unit cell (HCP),

$$\theta \sim \theta_1 = \frac{3\sqrt{3}c}{2a} = 4.1239, \text{ structural factor (HCP),}$$

$$\gamma = 1 + \frac{4\mu_1}{3\kappa} \sim 2,$$

$$C = \frac{(R_2^3 - R_1^3)}{3R_1^3 \gamma_2} = 0.09, \text{ misfit factor,}$$

and the equation,  $a = [a_1^3 + 4\pi R_1^3 x \frac{k_1}{\theta_1} \gamma C]^{\frac{1}{3}} \cdot [\frac{k\theta_1}{k_1\theta}]^{\frac{1}{3}}$ ,

when  $x = 4.228\text{ at\%}$ ,  $a = 2.97\text{ Å}$ ,  $c = 4.69\text{ Å}$ ;

when  $x = 13.390\text{ at\%}$ ,  $a = 3.02\text{ Å}$ ,  $c = 4.71\text{ Å}$

It gives a much better fit of lattice constant than Vegard’s law and has a maximum deviation of 2.37%.

4.3. Texture evolution

Twins generated during deformation can be clearly observed with optical microscope. The micro-structure of starting materials in rolling direction is shown below as Fig. 13.

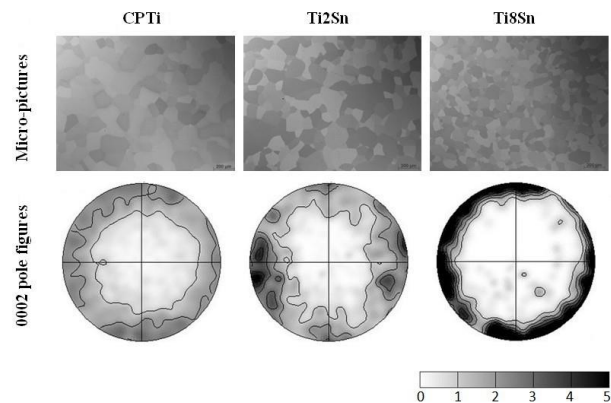


Fig. 13. Microstructure and 0002 pole figures of starting materials in RD.

For the starting materials, grain size was kept similar

(about  $80\mu\text{m}$ ). However  $\text{Ti}_8\text{Sn}$  exhibits a smaller grain size than pure titanium and  $\text{Ti}_2\text{Sn}$ . The (0002) pole figures for all the three alloys are quite similar which means the crystallographic orientation is similar. All of three alloys have a ring-shaped texture, indicating the c-axis of most grains is perpendicular to rolling direction.

As deformation strain along rolling direction increases, the c-axis is stretched. As a result, {1012} plane is highly possible to generate a twin in direction  $\langle 1011 \rangle$ . This is one kind of the tensile twin and this type of twin has a misorientation of about  $85^\circ$  with parent grain. When strain keeps increasing to 3.7%, the micro-structure of three alloys is shown below as Fig. 14.

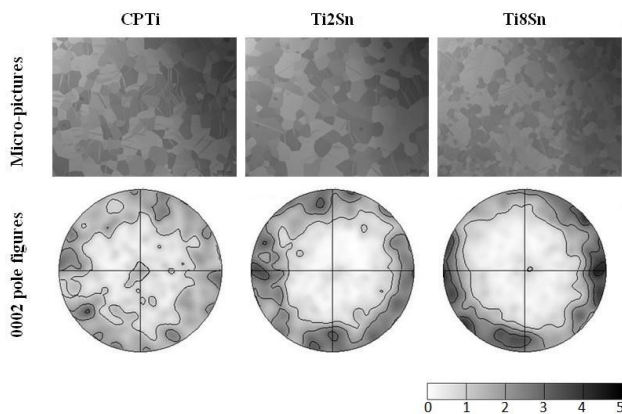


Fig. 14. Microstructure and 0002 pole figures of samples after 3.7% strain in RD.

After 3.7% strain is achieved, pure titanium exhibits massive twins in micrographs.  $\text{Ti}_2\text{Sn}$  and  $\text{Ti}_8\text{Sn}$  have similar twinning activity and the number of twin is much less than pure titanium. This can also be observed from the pole figures. In (0002) pole figure of pure titanium, there is some intensity of orientation emerged after deformation. This indicates many grains have rotated about  $90^\circ$  during deformation and now their c-axis is parallel to rolling direction. Massive tensile twin is activated. However for  $\text{Ti}_2\text{Sn}$  and  $\text{Ti}_8\text{Sn}$ , there is little intensity in centre of pole figures. Only a few grains have rotated, meaning only a few tensile twins are activated.

## 5. Conclusion

In this project three different orientations (rolling direction, normal direction and  $45^\circ$ ) are investigated and compared to characterise the orientation effect in titanium-tin alloying system. The results show that the difference between three orientations is negligible especially in hardness tests and twin area fraction. As a result all the materials are deemed to be homogeneous.

All the mechanical tests indicate that  $\text{Ti}_2\text{Sn}$  and  $\text{Ti}_8\text{Sn}$  have very similar properties which are quite different from pure titanium including higher hardness value and yield stress. Alloying effect of tin is remarkable at beginning and getting less at higher tin concentration.

In the lattice constant characterisation, with tin content increases,  $\langle a \rangle$  value stays nearly constant while  $\langle c \rangle$  value increase linearly.

Different twin systems as well as slip systems were observed during mechanical deformation. Twinning systems get harder to be activated with higher tin concentration.

As a conclusion, tin can greatly change the properties of titanium alloys like hardness, yield stress, lattice constant and mechanical behaviour.

## References

- [1] Lutjering Gerd, James C. Williams, Titanium, 2nd edition, Springer, 2007.
- [2] C. Leyens, M. Peters, Titanium and Titanium Alloys, WILEY-VCH Verlag GmbH & Co. KGaA, Weinheim, 2003.
- [3] Keytometal, Corrosion of Titanium and Titanium Alloys, 2009.
- [4] R. A. Higgins, Materials for engineers and technicians, Newnes, 2006.
- [5] V. A. Lubarda, Mechanics of Materials **35**(53–68), 53 (2003).
- [6] A. Mudar, Abdulsattar, Solid State Sci. **13**, 843 (2011).
- [7] H. R Wenk, P. Van Houtte (2004), Texture and anisotropy. Rep. Progr. Phys. 67: 1367–1428. Bibcode:2004RPPh...67.1367W.

\*Corresponding author: jiyinze@qq.com